Ice Formation in $(NH_4)_2SO_4-H_2O$ Particles

Allan K. Bertram, Thomas Koop,† Luisa T. Molina, and Mario J. Molina*

Department of Chemistry and Department of Earth, Atmospheric and Planetary Sciences, Massachusetts Institute of Technology, Cambridge, Massachusetts 02139

Received: September 2, 1999; In Final Form: November 9, 1999

Ice nucleation in upper tropospheric aerosols is believed to be a key step in upper tropospheric cloud formation, and therefore knowledge of the conditions leading to ice formation in these aerosols is crucial. This paper addresses homogeneous nucleation of ice in $(NH_4)_2SO_4-H_2O$ aerosols, a possible upper tropospheric aerosol. Two complementary techniques were employed in this study. First, differential scanning calorimetry was used to determine the temperature at which ice nucleates in emulsified solutions of ammonium sulfate and water. Second, optical microscopy was used to determine the temperature at which ice nucleates in individual ammonium sulfate−water particles. The results from these two techniques, which are in very good agreement, indicate that the freezing temperature of ammonium sulfate−water particles (approximately 10 μm in size) ranges from 235 K for 0 wt % to 195 K for 40 wt %. These freezing temperatures correspond to saturation ratios with respect to ice ranging from 1.45 at 235 K to 1.68 at 195 K, which are similar to the saturation ratios required for homogeneous freezing of $H_2SO_4-H_2O$ and $(NH_4)HSO_4-H_2O$ particles. Based on these saturations, we conclude that both homogeneous and heterogeneous nucleation are important in upper tropospheric cloud formation.

1. Introduction

Upper tropospheric clouds play an important role in the earth's climate[1,2] and in the chemistry of the upper troposphere.[3−5] These clouds form when ice precipitates in or on upper tropospheric aerosols.[6−9] Until recently it was generally assumed that these aerosols were mainly composed of H_2SO_4 and H_2O.[10,11] As a result, researchers have investigated the conditions required for homogeneous nucleation of ice in $H_2SO_4-H_2O$ particles.[12−14] Recent field work, however, has identified NH_4^+ ions in the upper troposphere, which suggests that the composition of these upper tropospheric aerosols can range from completely acidic (H_2SO_4 and H_2O) to completely neutralized [$(NH_4)_2SO_4$ and H_2O].[15] Consequently, knowledge of the conditions under which ice precipitates in partially neutralized and completely neutralized sulfate particles is highly desirable for the modeling of upper tropospheric clouds.[16,17]

In this paper, we report the conditions required for homogeneous nucleation of ice in $(NH_4)_2SO_4-H_2O$ particles (completely neutralized sulfuric acid−water particles). Two complementary techniques were employed in this study. Differential scanning calorimetry (DSC) was used to measure the temperature at which ice nucleates in aqueous ammonium sulfate−oil emulsions, and optical microscopy was used to measure the temperatures at which ice nucleates in individual ammonium sulfate−water particles.

2. Experimental Section

A brief discussion of the two experimental techniques used in this study is given here; full details have been given elsewhere.[14,18]

2.1. DSC of Emulsions. In the first set of experiments, we investigated ice formation in aqueous ammonium sulfate−oil emulsions; that is, micron-sized $(NH_4)_2SO_4-H_2O$ droplets suspended in an inert oil matrix. These emulsions were prepared by combining 0.2 mL of a $(NH_4)_2SO_4-H_2O$ solution with 2.5 mL of an oil phase and shaking the resulting mixture with a high speed mixer (Thermolyne Maxi-Mix III, type 65800) for 8 min. Using optical microscopy, we determined droplet sizes in several of the emulsions: the average diameter ranged from 5.6 to 11.0 μm, and the standard deviation from 2.1 to 5.9 μm.

The bulk solutions of $(NH_4)_2SO_4$ and H_2O used in the emulsion work were prepared by adding deionized water to 99.9% $(NH_4)_2SO_4$ crystals (Aldrich Chemical). The uncertainty in composition of the bulk solutions, and hence the uncertainty in the compositions of the droplets, is estimated to be $\pm$0.1 wt %. The oil phase used in the emulsions consisted of approximately 80 wt % halocarbon oil series 0.8 (Halocarbon Products Corporation) and 20 wt % lanolin (Aldrich Chemical).

Differential scanning calorimetry (DSC) was used to determine the thermal behavior of the emulsified $(NH_4)_2SO_4-H_2O$ solutions. The DSC technique involved monitoring the differential energy required to keep both a sample (emulsion) and a reference (oil−lanolin mixture) at the same temperature while the average temperature was varied at a constant rate (5 K/min). A commercial Perkin-Elmer DSC-7 instrument, calibrated with pure water (melting point at 273.15 K) and a water−methanol mixture (eutectic melting temperature at 168.65 K), was used for these measurements. The uncertainty in the melting temperatures and freezing temperatures after calibration is estimated to be $\pm$1.5 K.

2.2. Particle Microscopy. Phase transitions of $(NH_4)_2SO_4-H_2O$ particles ranging in size from 10 to 55 μm were observed with a Zeiss Axioskop 20 microscope equipped with 10× and 50× objectives. The microscope was modified to include a Linkam BCS 196 cold stage that housed a microcell (total

* To whom correspondence should be addressed.
† Current Address: Swiss Federal Institute of Technology, Atmospheric Physics, Hoenggerberg HPP, 8093 Zurich, Switzerland.

10.1021/jp9931197 CCC: $19.00
Published on Web 12/31/1999

volume of 3.5×10^{-4} cm^3). The bottom surface of this cell, made out of glass, was treated with an organosilane (Prosil 28) to reduce the possibility of heterogeneous nucleation initiated by the surface. The particles under investigation were deposited on the bottom surface of this cell with a nebulizer. Temperature calibration was performed by measuring the melting points of droplets or thin films of water (273.15 K), dodecane (263.55 K), octane (216.35 K), and toluene (178.15 K).

A typical freezing experiment consisted of cooling the microcell at a rate of 10 K/min to approximately 173 K. A cooling rate of 10 K/min was needed to reduce mass transfer between frozen particles and unfrozen particles. Thereafter, the temperature of the cell was increased at a rate of 1 K/min until all of the particles were completely melted.

Typically, 20−30 droplets were monitored simultaneously during an experiment. All experiments were recorded on tape via the attached video system, and the tape was evaluated afterward to determine the freezing and melting temperature of each droplet. The concentration of each particle was determined by converting the melting temperature into composition using the thermodynamic model of Clegg et al.[19] The uncertainty in determining the composition is estimated to be ±1.0 wt %, based on the uncertainty in determining the melting temperature. From the freezing temperatures and concentrations of the individual droplets, the average concentration and median freezing temperature was determined for each experiment. We chose to calculate the median freezing temperature and not the average freezing temperature because heterogeneous nucleation by a small fraction of the total drops has a much smaller impact on the median freezing temperature than on the average freezing temperature.

3. Results

3.1. DSC Results. DSC thermograms were recorded for emulsified $(NH_4)_2SO_4-H_2O$ solutions with compositions ranging from 0 to 42 wt %. Shown in Figure 1(a) are cooling thermograms of 10.0, 15.3, and 20.1 wt % $(NH_4)_2SO_4$ samples. Over the entire concentration range investigated, only one peak was observed in each cooling thermogram. This peak, which corresponds to the nucleation and freezing of the aqueous drops, shifted to lower temperatures as the concentration of $(NH_4)_2SO_4$ increased. By assuming that the area under these peaks is directly proportional to the fraction of total droplet mass that crystallized, we determined the fraction of total mass frozen as a function of temperature. Shown in Figure 2 are the temperatures at which 50% of the total droplet mass is frozen (solid circles). Note that these freezing temperatures do not change significantly if a different percentage is used to represent the freezing data. For example, the difference in temperatures between 10% and 50% frozen is on average 1.5 K, while the difference in temperatures between 50% and 90% frozen is on average 1.1 K.

In contrast to the cooling thermograms, two peaks were observed in the heating thermograms. Shown in Figure 1(b) are heating thermograms of 10.0, 15.3, and 20.1 wt % $(NH_4)_2SO_4$ samples. The low temperature peaks in the heating thermograms correspond to melting at the eutectic, whereas the higher temperature peaks correspond to melting at the ice−liquid equilibrium temperatures. The melting temperatures were determined by extrapolating the melting peaks to the baseline of the thermograms. The results of this analysis for compositions ranging from 0 to 42 wt % are displayed in Figure 2. The open circles represent the eutectic temperatures and the open triangles represent the ice−liquid equilibrium temperatures. The ice−liquid equilibrium temperatures for concentrations greater than 30 wt % were not determined because of the overlap between the ice peak and the eutectic peak. Also shown in Figure 2 is the ice−liquid equilibrium curve, the crystalline $(NH_4)_2SO_4$−liquid equilibrium curve, and the eutectic line, all of which were calculated with the model by Clegg et al.[19] The good agreement between the calculations and the measured melting temperatures confirms the accuracy of our method of determining the droplet composition.

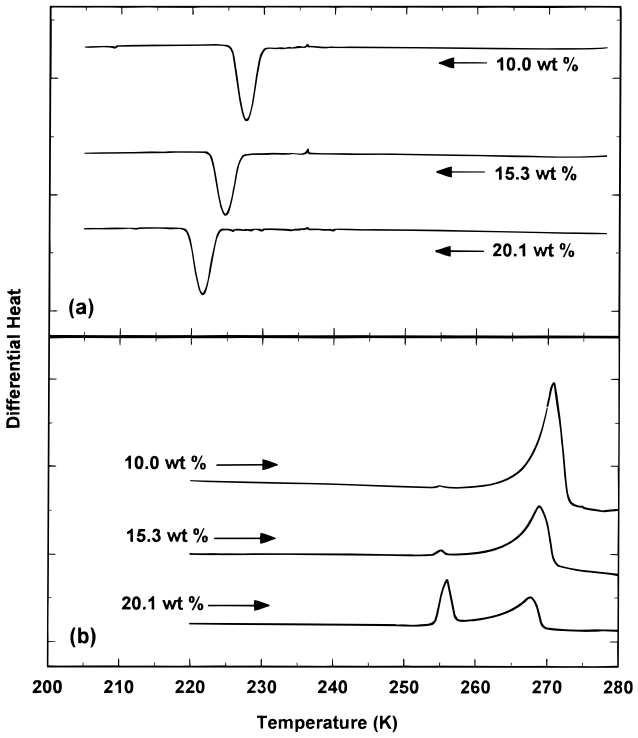

Figure 1. DSC thermograms of aqueous ammonium sulfate−oil emulsions (the concentration of ammonium sulfate in weight percent is indicated in the figure). The three curves in (a) correspond to cooling experiments, and the three curves in (b) correspond to heating experiments. The arrows indicate the direction of temperature change.

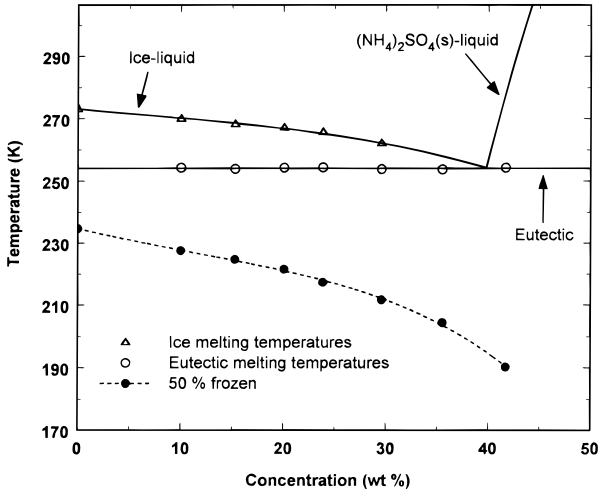

Figure 2. Results from the DSC experiments. The solid circles indicate the temperature at which 50% of the total aqueous mass of the emulsions froze. The open circles indicate the measured eutectic temperatures, and the open triangles indicate the measured ice−liquid equilibrium temperatures. The solid lines are the ice−liquid, $(NH_4)_2SO_4$−liquid, and eutectic equilibrium temperatures, calculated with a thermodynamic model by Clegg et al.[19]

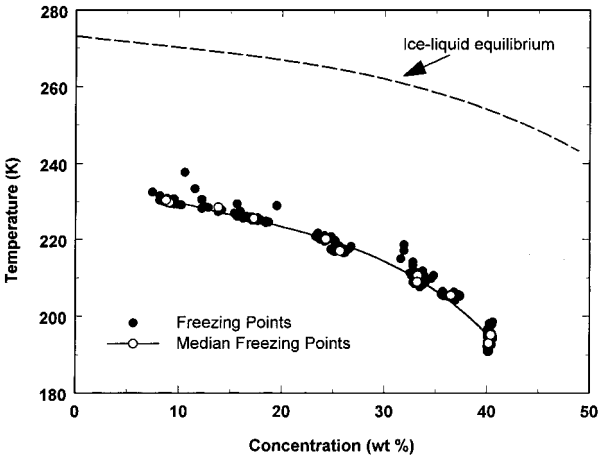

Figure 3. Results from the microscope experiments. The solid circles are the freezing temperatures determined for individual particles and the open triangles are the median freezing temperatures. The solid line is the best fit to the median freezing temperatures. The long dashed line is the ice−liquid equilibrium curve.

3.2. Microscope Results. The freezing temperatures of $(NH_4)_2SO_4-H_2O$ particles were also measured using optical microscopy. The results are displayed in Figure 3. The open circles correspond to the median freezing temperatures and average concentrations, and the solid line through the open circles is the result of a least-squares analysis of these data. The solid circles shown in Figure 3 are the raw data used to determine the median freezing temperatures and average concentrations. Each solid point corresponds to a freezing temperature and concentration of an individual particle. The scatter in these points is mainly due to the stochastic nature of homogeneous nucleation. In addition, heterogeneous nucleation probably initiated freezing in the few particles that froze at temperatures significantly higher than the median freezing temperatures. This, however, does not have a significant impact on our median freezing temperatures, as discussed above. The uncertainty in the median freezing temperatures is approximately ±1.5 K.

4. Discussion

The results from the microscope and DSC freezing experiments displayed in Figures 2 and 3 are compared in Figure 4. The open circles are the median freezing temperatures determined in the microscope experiments. The solid circles are the temperatures at which 50% of the total droplet mass froze in the DSC experiments. The agreement between the two sets of data is quite good, which suggests that neither the surface in contact with the particles in the microscope experiments nor the oil phase in the emulsion experiments affected the nucleation process. The short dashed curve shown in Figure 4 is the result of a least-squares fit to both the microscope and DSC results. The parameters that describe this curve are given in Table 1.

Also shown in Figure 4 are results from Cziczo and Abbatt, the only other study of homogeneous nucleation of $(NH_4)_2SO_4-H_2O$ reported in the literature.[20] Using infrared spectroscopy, these authors investigated the freezing of $(NH_4)_2SO_4-H_2O$ particles less than 1 μm in size suspended in a buffer gas. The solid diamonds are the temperatures at which they first observed freezing. The agreement between our data and the Cziczo and Abbatt data is good at concentrations less than 15 wt %. At higher concentrations, however, our results show significantly lower freezing temperatures than Cziczo and Abbatt: at 42 wt %, a difference of approximately 30 K is apparent. This

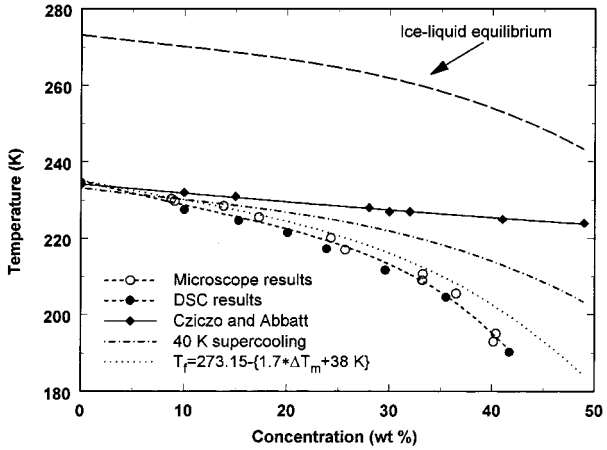

Figure 4. Comparison of our DSC and microscope freezing points with other data. The solid circles represent the DSC results, and the open circles represent the microscope results. The short dashed line is a fit to both the microscope and DSC results. The diamonds represents the results from Cziczo and Abbatt,[20] and the solid line through the Cziczo and Abbatt data is the result of a least-squares analysis. The dashed−dotted line represents a constant 40 K supercooling, and the dotted line represents a mathematical expression previously used to predict freezing of ammonium sulfate−water particles.[24,25]

TABLE 1: Freezing Temperature as a Function of $(NH_4)_2SO_4$ Concentration

	A_0	A_1	A_2	A_3
T^*	235.15	−0.70305	7.1221×10^{-3}	-9.0405×10^{-6}

T^* can be calculated from $T^* = A_0 + A_1wt + A_2wt^2 + A_3wt^4$, where T^* is the freezing temperature (in K) and wt is the $(NH_4)_2SO_4$ concentration (in wt %). These parameters are valid from 0 to 42 wt % $(NH_4)_2SO_4$.

discrepancy cannot be explained by differences in particle size, since the particles investigated by Cziczo and Abbatt were smaller than the particles investigated in this work, and the freezing temperature of particles of the same composition decrease slightly with particle size.[21] Additional experiments are needed to explain the discrepancy; we can only speculate that it is related to the methods of determining the composition of the particles. In both the DSC experiments and the microscope experiments, composition determination is rather straightforward. Determination of the particle composition using the flow tube and FTIR technique, however, is inherently more difficult.

Previously, it was suggested that aqueous solution particles supercool by 40 K below the ice−liquid equilibrium melting temperature irrespective of the particle concentration.[22] In Figure 4, a constant 40 K supercooling (dashed−dotted curve) is compared with our microscope and DSC freezing results. Clearly, the 40 K curve underestimates the supercooling of $(NH_4)_2SO_4-H_2O$ particles at concentrations greater than 20 wt % $(NH_4)_2SO_4$.

The following mathematical expression, which is based on emulsion experiments of NH_4F, NH_4Cl, NaCl, and NaF aqueous solutions,[23] has also been used in the past to predict the freezing temperatures of $(NH_4)_2SO_4-H_2O$ particles:[24,25]

$$T_f = 273.15 - (1.7\Delta T_m + \Delta T_{H2O}) \qquad (1)$$

where T_f is an effective freezing temperature (in Kelvin), ΔT_m is the equilibrium melting point depression for a specific salt concentration, and ΔT_{H2O} is the supercooling of pure water droplets. In Figure 4 we compare this expression (dotted curve) to our freezing data by setting $\Delta T_{H2O} = 38$ K. Fixing ΔT_{H2O} at 38 K makes the original expression valid for particles of a few

TABLE 2: Critical Ice Nucleation Parameters, X^*, as a Function of the Water Vapor Pressure, P_{H2O}, for Micron-Sized $(NH_4)_2SO_4-H_2O$ Droplets

X^*	A_0	A_1	A_2	A_3	A_4	A_5
T^*	2.503×10^2	1.139×10^1	8.034×10^{-1}	8.666×10^{-2}	7.08×10^{-3}	2.47×10^{-4}
S_{ice}^*	1.263×10^0	-1.782×10^{-1}	-4.755×10^{-2}	-8.599×10^{-3}	-7.86×10^{-4}	-2.66×10^{-5}
a_w^*	1.016×10^0	-1.820×10^{-2}	-2.842×10^{-2}	-6.298×10^{-3}	-6.05×10^{-4}	-2.18×10^{-5}
ΔT^*	-2.531×10^0	9.835×10^{-1}	3.693×10^{-1}	6.796×10^{-2}	6.39×10^{-3}	2.36×10^{-4}

X^* can be calculated from $X^* = A_0 + A_1(\ln P_{H2O}) + A_2(\ln P_{H2O})^2 + A_3(\ln P_{H2O})^3 + A_4(\ln P_{H2O})^4 + A_5(\ln P_{H2O})^5$, where P_{H2O} is the water vapor pressure (in mb). T^* is the critical temperature (in K). S_{ice}^* is the critical ice saturation ratio. a_w^* is the critical water activity. ΔT^* is the critical supercooling (in K).

microns in size, the approximate size used in our experiments. The resulting freezing curve is in good agreement with our freezing data but slightly underestimates the supercooling at high concentrations. We suggest that the freezing temperatures are better represented by the parameters given in Table 1, the results of a least-squares analysis of our freezing data.

5. Atmospheric Implications

Based on our particle sizes and cooling rates, we estimate that our freezing curve (Figure 4, dashed line) corresponds to the temperatures and concentrations at which the homogeneous nucleation rate of ice is approximately 3×10^8 $cm^{-3}sec^{-1}$.[21] The nucleation rate required to freeze 10% of the particles in a typical aerosol in the upper troposphere is approximately 10^{11} $cm^{-3}sec^{-1}$. Consequently, the temperature required to freeze 10% of the particles in an upper tropospheric aerosol will be lower than the temperatures displayed in Figure 4. On the other hand, even small temperature changes lead to very large changes in the homogeneous nucleation rate of ice in dilute solutions.[21] Hence, our freezing curve, to a first approximation, should be directly comparable to the field data.

One of the most convenient parameters for comparing particle freezing temperatures measured in the laboratory with field data is the critical ice saturation (the ice saturation ratio required for freezing). The critical ice saturation is defined by the following equation:

$$S_{ice}^*(T) = P_{H2O}^*(T)/P_{ice}(T) \quad (2)$$

where $S_{ice}^*(T)$ is the critical ice saturation at the freezing temperature T, $P_{H2O}^*(T)$ is the equilibrium partial pressure of water over liquid $(NH_4)_2SO_4-H_2O$ at the freezing temperature, and $P_{ice}(T)$ is the vapor pressure of ice also at the freezing temperature.

Using the model of Clegg et al. and our freezing data, we have calculated S_{ice}^* as a function of water vapor pressure. The results of these calculations are presented in Table 2. The following parameters were also calculated as a function of water vapor pressure for comparison with field data: the critical water activity (a_w^*), the freezing temperature (T^*), and the cooling below the ice frost point (ΔT^*). These parameters are also included in Table 2.

Note that the parameters shown in Table 2 do not apply to particles smaller than approximately 0.1 μm. For these sizes, the Kelvin effect becomes important, and, hence, the parameters shown in Table 2 provide only an upper limit for T^* and a lower limit for S_{ice}^*, a_w^*, and ΔT^*. Most upper tropospheric aerosols, however, contain a significant amount of particles larger than 0.1 μm. These larger particles will most likely freeze first and induce cloud formation. Consequently, the parameters quoted in Table 2 can be used to approximate the freezing of upper tropospheric aerosols and cirrus cloud formation.

Shown in Figure 5 are critical ice saturation ratios as a function of temperature. The solid circles are the critical ice saturation ratios required for freezing of ammonium sulfate−water particles, calculated from our DSC and microscope freezing results. The solid line through the data points was calculated with the parameters displayed in Table 2. The uncertainty in S_{ice}^* associated with this curve is estimated to be ± 0.05, based on the uncertainties in the measured freezing temperatures. Also shown in Figure 5 are critical ice saturations required for freezing of $H_2SO_4-H_2O$ particles[14] [short dashed line] and $(NH_4)HSO_4-H_2O$ particles[26] [long dashed line] that have been previously measured in this laboratory. The uncertainty associated with these curves is also estimated to be ± 0.05. The critical ice saturations shown in Figure 5 are very similar in all three cases: the saturation required for freezing increases with decreasing temperature, and large saturations are required for freezing regardless of the concentration. Such large saturations have been observed in the upper tropospheric region. For example, saturations of approximately 1.6 at 209 K have been observed in upper tropospheric wave clouds,[27,28] indicating that homogeneous nucleation is occurring. Much lower saturations, however, have also been observed. For example, Heymsfield et al.[28,29] measured values of approximately 1.3 at 220 K during several campaigns. Our laboratory measurements indicate that a saturation of at least 1.53 must be reached in order for homogeneous nucleation to occur at this temperature. These two sets of results suggest that heterogeneous nucleation is occurring in these clouds. We conclude that both homogeneous nucleation and heterogeneous nucleation are important processes in upper tropospheric cloud formation. To accurately assess the relative importance of these two mechanisms, more measurements of critical ice saturations in the upper tropospheric region are needed.

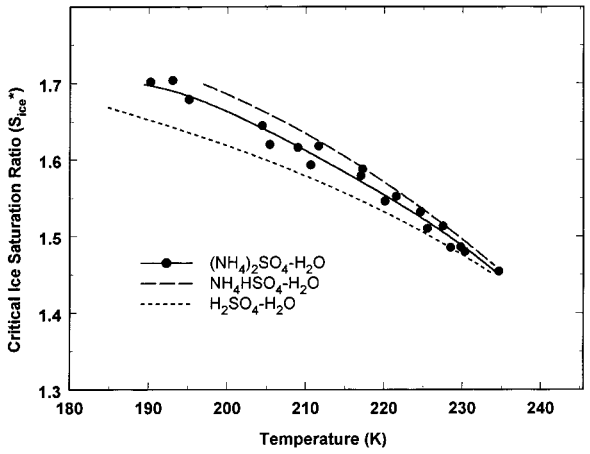

Figure 5. Critical ice saturations required for homogeneous nucleation of various aqueous aerosols. The solid line and solid circles correspond to ammonium sulfate and water (this work). The dashed line corresponds to sulfuric acid and water (Koop et al.[14]), and the long dashed line corresponds to ammonium bisulfate and water (Koop et al.[26]).

6. Conclusions

Differential scanning calorimetry and optical microscopy were used to determine the temperature at which ice nucleates in ammonium sulfate−water particles. The results from the two techniques are in very good agreement, which suggests that both are capable of determining freezing properties of solution droplets. The results from this study reveal that a supercooling of 59 K at 40 wt % is needed to form ice, which is higher than expected based on previous laboratory measurements and theoretical considerations.

Using a thermodynamic model, we determined that the ice saturation required for homogeneous nucleation of ammonium sulfate−water particles ranges from 1.45 at 235 K to 1.68 at 195 K. These saturations are similar to the saturations required for homogeneous freezing of $H_2SO_4-H_2O$ and $(NH_4)HSO_4-H_2O$ particles, and are sometimes larger than observed during field campaigns in the upper tropospheric region. We conclude that both homogeneous nucleation and heterogeneous nucleation are important processes in upper tropospheric cloud formation.

Acknowledgment. This work was supported by grants from NASA's Atmospheric Effects of Aviation Program and the National Science Foundation. A.K.B. acknowledges a Natural Science and Engineering Research Council of Canada Postdoctoral Fellowship, and T.K. acknowledges a Feodor Lynen Fellowship from the Humboldt Foundation and an Otto Hahn Fellowship from the Max Planck Society. We thank S. Clegg for providing us with a code for his thermodynamic model, and also J. Abbatt and D. Cziczo for sending us a preprint of their work.

References and Notes

(1) Ramanathan, V.; Pitcher, E. J.; Malone, R. C.; Blackman, L. *J. Atmos. Sci*. **1983**, *40*, 605.
(2) Liou, K. N. *Mon. Weather Rev*. **1986**, *114*, 1167.
(3) Reichardt, J.; Ansmann, A.; Serwazi, M.; Weitkamp, C.; Michaelis, W. *Geophys. Res. Lett*. **1996**, *23*, 1929.
(4) Borrmann, S.; Solomon, S.; Dye, J. E.; Luo, B. P. *Geophys. Res. Lett*. **1996**, *23*, 2133.
(5) Kley, D.; Crutzen, P. J.; Smit, H. G. J.; Vomel, H.; Oltmans, S. J.; Grassl, H.; Ramanathan, V. *Science* **1996**, *274*, 230.
(6) Jensen, E. J.; Toon, O. B.; Westphal, D. L.; Kinne, S.; Heymsfield, A. J. *J. Geophys. Res*. **1994**, *99*, 10421.
(7) Heymsfield, A. J.; Sabin, R. M. *J. Atmos. Sci*. **1989**, *4*, 2252.
(8) Sassen, K.; Dodd, G. C. *J. Atmos. Sci*. **1989**, 46, 3005.
(9) Demott, P. J.; Meyers, M. P.; Cotton, W. R. *J. Atmos. Sci*. **1994**, *51*, 77.
(10) Seinfeld, J. H. *Nature* **1998**, *391*, 837.
(11) Sheridan, P. J.; Brock, C. A.; Wilson, J. C. *Geophys. Res. Lett*. **1994**, *21*, 2587.
(12) Bertram, A. K.; Patterson, D. D.; Sloan, J. J. *J. Phys. Chem*. **1996**, *100*, 2376.
(13) Clapp, M. L.; Niedziela, R. F.; Richwine, L. J.; Dransfield, T.; Miller, R. E.; Worsnop, D. R. *J. Geophys. Res*. **1997**, *102*, 8899.
(14) Koop, T.; Ng, H. P.; Molina, L. T.; Molina, M. J. *J. Phys. Chem. A* **1998**, *102*, 8924.
(15) Talbot, R. W.; Dibb, J. E.; Loomis, M. B. *Geophys. Res. Lett*. **1998**, *25*, 1367.
(16) Martin, S. T. *Geophys. Res. Lett*. **1998**, *25*, 1657.
(17) Tabazadeh, A. *Geophys. Res. Lett*. **1998**, *25*, 1379.
(18) Chang, H. A.; Koop, T.; Molina, L. T.; Molina, M. J. *J. Phys. Chem. A* **1999**, *103*, 2673.
(19) Clegg, S. L.; Brimblecombe, P.; Wexler, A. S. *J. Phys. Chem. A* **1998**, *102*, 2137.
(20) Cziczo, D. J.; Abbatt, J. P. D. *J. Geophys. Res*. **1999**, *104*, 13781.
(21) Pruppacher, H. R.; Klett, J. D. *Microphysics of Clouds and Precipitation*, 2nd ed.; Kluwer: Dordrecht, 1997.
(22) Hallett, J.; Lewis, R. E. S. *Weather* **1967**, *22*, 56.
(23) Rasmussen, D. J. *J. Cryst. Growth* **1982**, *56*, 56.
(24) Sassen, K.; Dodd, G. C. *J. Atmos. Sci*. **1988**, *45*, 1357.
(25) DeMott, P. J.; Meyers, M. M.; Cotton, W. R. *J. Atmos. Sci*. **1994**, *51*, 77.
(26) Koop, T.; Bertram, A. K.; Molina, L. T.; Molina, M. J. *J. Phys. Chem. A* **1999**, *103*, 9042.
(27) Jensen, E. J.; Toon, O. B.; Tabazadeh, A.; Sachse, G. W.; Anderson, B. E.; Chan, K. R.; Twohy, C. W.; Gandrud, B.; Aulenbach, S. M.; Heymsfield, A.; Hallett, J.; Gary, B. *Geophys. Res. Lett*. **1998**, *25*, 1363.
(28) Heymsfield, A. J.; Miloshevich, L. M.; Twohy, C.; Sachse, G.; Oltmans, S. *Geophys. Res. Lett*. **1998**, *25*, 1343.
(29) Heymsfield, A. J.; Miloshevich, L. M. *J. Atmos. Sci*. **1995**, 52, 4302.